

# Atomic Force Microscopy Imaging of TiO<sub>2</sub> Surfaces Active for C-C Bond Formation Reactions in Ultrahigh Vacuum

Brian A. Watson and Mark A. Barteau\*

Center for Catalytic Science and Technology, Department of Chemical Engineering,  
University of Delaware, Newark, Delaware 19716

Received December 16, 1993. Revised Manuscript Received April 4, 1994\*

TiO<sub>2</sub> (001) single crystal surfaces active for a variety of different chemistries were examined using atomic force microscopy (AFM). C-C bond forming reactions previously identified on these surfaces include carboxylic acid ketonization, aldol condensation, reductive carbonyl coupling, and alkyne cyclotrimerization. The surfaces were prepared in ultrahigh vacuum (UHV) and examined by AFM in air. Surfaces examined included the {011}-faceted surface, {114}-faceted surface, and argon-ion-bombarded surfaces, as well as the mechanically polished single-crystal surface prior to treatment in UHV. The one unifying feature of all the images was their extreme flatness. Root-mean-square roughnesses were routinely less than 10 Å in 500 × 500 nm scans. These same scans showed the surfaces to have surface areas exceeding that of an ideal flat surface by no more than 1.2%. Images of the polished surface revealed a variety of surface features, including polishing scratches and particle-like features. The argon-ion-bombarded surface and the faceted surfaces were composed of large flat plateaus ranging in size from 21 to 75 nm. The size of the plateaus was essentially the same for the ion bombarded surface and the {011}-faceted surface. The {114}-faceted surface exhibited slightly smaller plateau regions than the other surfaces. The images indicate that argon-ion bombardment, while disordering the surface and causing significant composition changes, does not lead to observable morphological changes on this scale. The relative uniformity of the surfaces examined is consistent with the selectivity of carbon-carbon bond-forming reactions that have been shown to take place on these surfaces. The images also reveal how the surface topography on the scale of the plateau structures observed is only slightly changed during the transformation of the surface unit cell structure from the {011}- to the {114}-faceted surface.

## Introduction

Thermodynamically driven to minimize surface free energy, many metals and metal oxides are known to form faceted structures. Since thermal faceting leads to surfaces that are structurally more complicated than simple terminations of the bulk lattice, surfaces with a tendency to facet are often avoided in surface science studies. However, provided that the faceted structures can be sufficiently well-characterized, these surfaces provide unique opportunities to probe the variation of chemical reactivity with progressive changes in structure of the same surface. TiO<sub>2</sub>(001) is one such metal oxide surface which undergoes several structural changes that yield faceted structures,<sup>1</sup> these have been shown to exhibit different activities and selectivities for a variety of surface reactions.<sup>2-6</sup>

The geometric and electronic structure of TiO<sub>2</sub>(001) surfaces has been characterized by several groups using LEED, UPS, and XPS.<sup>1,7-9</sup> On the basis of LEED experiments, Firment has identified two distinct phases

that form on the (001) surface of TiO<sub>2</sub> upon annealing.<sup>1</sup> The "low-temperature phase"<sup>1</sup> forms upon annealing at 750 K.<sup>3</sup> This surface has been described as "{011}-faceted," with each titanium cation in the ideal structure 5-fold coordinated to oxygen anions.<sup>1</sup> The titanium cations remain in the +4 oxidation state as indicated by XPS measurements.<sup>4,9</sup> Annealing at 950 K produces a "{114}-faceted" structure<sup>1</sup> in which surface titanium +4 cations are coordinated to 4, 5, or 6 oxygen anions. Ion bombardment disorders these surfaces.<sup>10</sup> Sputtering preferentially depletes the surface of oxygen, thus reducing the surface. Titanium cations in the +1, +2, +3, and +4 oxidation states have been detected on sputter-reduced surfaces by XPS.<sup>9,11-14</sup>

We have shown that a surprising variety of carbon-carbon bond-forming reactions take place even in UHV on the various TiO<sub>2</sub>(001) surfaces described above.<sup>2-5,15-17</sup> On the oxidized, {114}-faceted surface, ketonization of carboxylic acid occurs. This reaction requires surface Ti<sup>4+</sup>

\* Abstract published in *Advance ACS Abstracts*, May 1, 1994.

- (1) Firment, L. E. *Surf. Sci.* **1992**, *116*, 205.
- (2) Barteau, M. A. *J. Vac. Sci. A* **1993**, *11*, 2162.
- (3) Kim, K. S.; Barteau, M. A. *Surf. Sci.* **1991**, *223*, 13.
- (4) Kim, K. S.; Barteau, M. A. *J. Catal.* **1990**, *125*, 353.
- (5) Idriss, H.; Kim, K. S.; Barteau, M. A. In *Structure-Activity Relationships in Heterogeneous Catalysis*; Grasselli, R. K., Sleight, A. W., Eds.; Elsevier: Amsterdam, 1991; p 327.
- (6) Kim, K. S.; Barteau, M. A. *Langmuir* **1990**, *6*, 1485.
- (7) Tait, R. H.; Kasowski, R. V. *Phys. Rev. B* **1979**, *20*, 5178.
- (8) Kasowski, R. V.; Tait, R. H. *Phys. Rev. B* **1979**, *20*, 5168.
- (9) Idriss, H.; Barteau, M. A. *Catal. Lett.*, in press.

(10) Hoflund, G. B.; Yin, H.-L.; Grogan, Jr., A. L.; Asbury, D. A.; Yoneyama, H.; Ikeda, O.; Tamura, H. *Langmuir* **1988**, *4*, 346.

(11) Göpel, W.; Anderson, J. A.; Frankel, D.; Jaehnic, M.; Phillips, K.; Schaefer, J. A.; Rucker, G. *Surf. Sci.* **1984**, *139*, 333.

(12) Carley, A. F.; Chalker, P. R.; Rivière, J. C.; Roberts, M. W. *J. Chem. Soc., Faraday Trans. 1* **1987**, *83*, 351.

(13) Sayers, C. N.; Armstrong, N. R. *Surf. Sci.* **1978**, *77*, 301.

(14) Rucker, G.; Göpel, W. *Surf. Sci.* **1987**, *181*, 530.

(15) Idriss, H.; Pierce, K.; Barteau, M. A. *J. Am. Chem. Soc.* **1991**, *113*, 715.

(16) Idriss, H.; Pierce, K. G.; Barteau, M. A. *J. Am. Chem. Soc.*, in press.

(17) Idriss, H.; Barteau, M. A. In *Heterogeneous Catalysis and Fine Chemicals III*; Guisnet, M., et al., Eds.; Elsevier: Amsterdam, 1983; p 463.

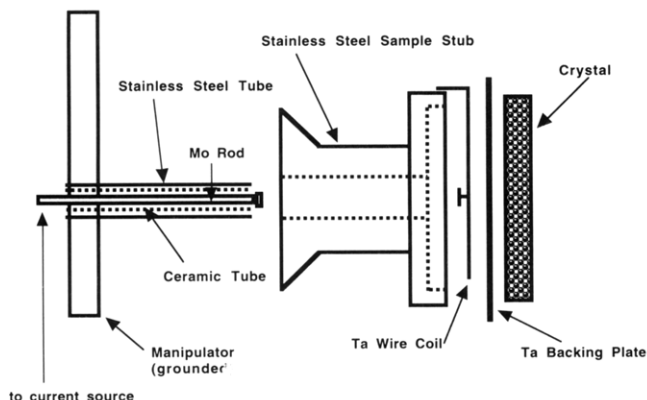


**Figure 1.** Schematic of the heatable sample stub and manipulator attachment.

cations with two coordination vacancies and is not observed on the {011}-faceted surface which does not provide such sites.<sup>3-5</sup> In contrast, aldol condensation of aldehydes occurs on both surfaces, requiring only sites for proton abstraction.<sup>18</sup> The reduced, argon-ion-bombarded surface can perform several classes of reductive coupling reactions with high selectivity, including coupling of aldehydes and ketones to form symmetric olefins<sup>15-17</sup> and the cyclotrimerization of alkynes to form alkyl benzenes.<sup>19</sup> Reductive carbonyl coupling requires an ensemble of surface cations collectively capable of effecting this four-electron reduction<sup>16</sup> while alkyne cyclotrimerization has been shown to occur at individual  $Ti^{2+}$  cation sites on the surface.<sup>19</sup>

Reactions which are sensitive to surface structure and oxidation state can be selected by changing the surface composition and structure via annealing and ion bombardment techniques. For example, the reductive coupling reactions above and others, including reductive oligomerization of benzoquinone, require reduced surfaces; the oxidized, faceted surfaces of  $TiO_2$  exhibit activities more than an order of magnitude lower for such reactions.<sup>16,17</sup> These studies of  $TiO_2(001)$  provide clear examples of how the site requirements for surface reactions can be investigated using differently prepared surfaces of the same metal oxide single crystal. High selectivities for site-specific reactions imply that the surface is relatively uniform. Sites not selective for the reaction of interest must be either absent or, if present, considerably less active for competing reaction pathways. LEED is one method for examining surface homogeneity. However, this technique provides details only of the long range order of the surface within the coherence length (typically ca. 100 Å) of the electron beam. Modest ion bombardment of ordered  $TiO_2(001)$  surfaces causes disorder and destroys the LEED pattern. However, the extent of disorder can not be ascertained from such experiments. The advent of scanning probe microscopies (SPM) such as scanning tunneling microscopy (STM) and atomic force microscopy (AFM) allows, for the first time, the direct investigation of surface structures down to the nanometer scale; sometimes with atomic resolution. Such techniques are therefore promising tools for assessing the structural uniformity of  $TiO_2(001)$  surfaces active for different chemistries.

SPM images of several well-defined  $TiO_2$  surfaces have been reported previously.<sup>20-24</sup> The (001) surface has been

studied by both AFM and STM.<sup>22-25</sup> Using STM under ultrahigh-vacuum (UHV) conditions Poirier et al. studied the {011}-faceted surface ("low-temperature phase").<sup>22</sup> Their study showed, in agreement with earlier LEED studies, that annealing at 783 K produced primarily {011} and stepped {011} facet planes on  $TiO_2(001)$ . The facet planes were described as 200-Å-wide crystallites (ranging from 100 to 500 Å) scattered about the surface. Their study also revealed surface features not detected by LEED, such as (001) terraces and (045) and (023) planes.

Lad and co-workers have reported characteristics of  $TiO_2(001)$  surfaces prepared in UHV and imaged with AFM in air.<sup>23-25</sup> The  $TiO_2(001)$  surfaces examined in those studies had been annealed at temperatures of 873, 1173, and 1573 K. The 873 K surface showed a diffuse ( $1 \times 1$ ) LEED pattern with faint evidence of faceting. This surface, which exhibited a root-mean-square (rms) roughness of 26 Å (for a 350 nm  $\times$  350 nm scan area), was covered with features approximately 500 Å wide and 20-30 Å tall. Annealing at 1173 K resulted in surfaces that were {011}-faceted as determined by LEED, with rms roughnesses of 68 Å after 1 h of annealing and 116 Å after 4 h. AFM images showed the facets to vary in size and orientation. Increased annealing times roughened the surface. Samples annealed at 1573 K did not facet but instead formed a network of ridges covering the surface. Such ridges had not been seen previously.

In this report we examine the surface morphology of  $TiO_2(001)$  surfaces active for the chemistries discussed above. These include the argon-ion-bombarded surface, {011}-faceted surface, and the {114}-faceted surface, as well as the polished surface prior to UHV preparation. The surfaces were prepared in UHV and imaged in air using AFM. As will be demonstrated, these surfaces exhibit considerably greater uniformity than previous images by other workers, consistent with the selective surface chemistry we have been able to carry out.

## Experimental Section

AFM experiments were carried out using a Digital Instruments Nanoscope III (NS III) Multimode scanning probe microscope and a Topometrix TMX 2010 scanning probe microscope. Images recorded with the NS III were obtained using the technique of tapping mode AFM (TMAFM) with single-crystal silicon cantilevers having a nominal tip radius of 100 Å. In TMAFM the cantilever is modulated by a piezoceramic, causing it to oscillate. The cantilever is a single crystal silicon pyramid which is generally operated near its resonance frequency (ca. several hundred kilohertz). To record an image, the cantilever is lowered to a position above the surface such that during the oscillation the cantilever briefly contacts the surface. By striking the surface the oscillation amplitude of the cantilever is reduced. An appropriate reduced amplitude is chosen as a set point. While the cantilever is rastered laterally, the  $z$  position ( $z$  direction chosen as perpendicular to the sample surface plane) of the sample is raised and lowered by a piezoceramic element to maintain the set point oscillation amplitude. By monitoring the change in  $z$  position of the sample, an image of the surface is produced. All images obtained with the Topometrix instrument were recorded using traditional contact AFM with silicon nitride tips having a nominal force constant of 0.064 N/m and tip radius of ca. 400 Å.

(21) Clark, G. W.; Kesmodel, L. L. *Ultramicroscopy* **1992**, *41*, 77.

(22) Poirier, G. E.; Hance, B. K.; White, J. M. *J. Vac. Sci. B* **1992**, *10*, 6.

(23) Lad, R. D.; Antonik, M. D. *Ceram. Trans.* **1991**, *24*, 359.

(24) Antonik, M. D.; Lad, R. D. *J. Vac. Sci. A* **1992**, *10*, 669.

(25) Antonik, M. D.; Edwards, J. C.; Lad, R. D. *Mater. Res. Soc. Symp. Proc.* **1992**, *237*, 459.

(18) Idriss, H.; Kim, K. S.; Barbeau, M. A. *J. Catal.* **1993**, *139*, 119.

(19) Pierce, K. G.; Barbeau, M. A. *J. Phys. Chem.* **1994**, *98*, 3882.

(20) Rohrer, G. S.; Henrich, V. E.; Bonnell, D. A. *Science* **1990**, *250*, 1239.

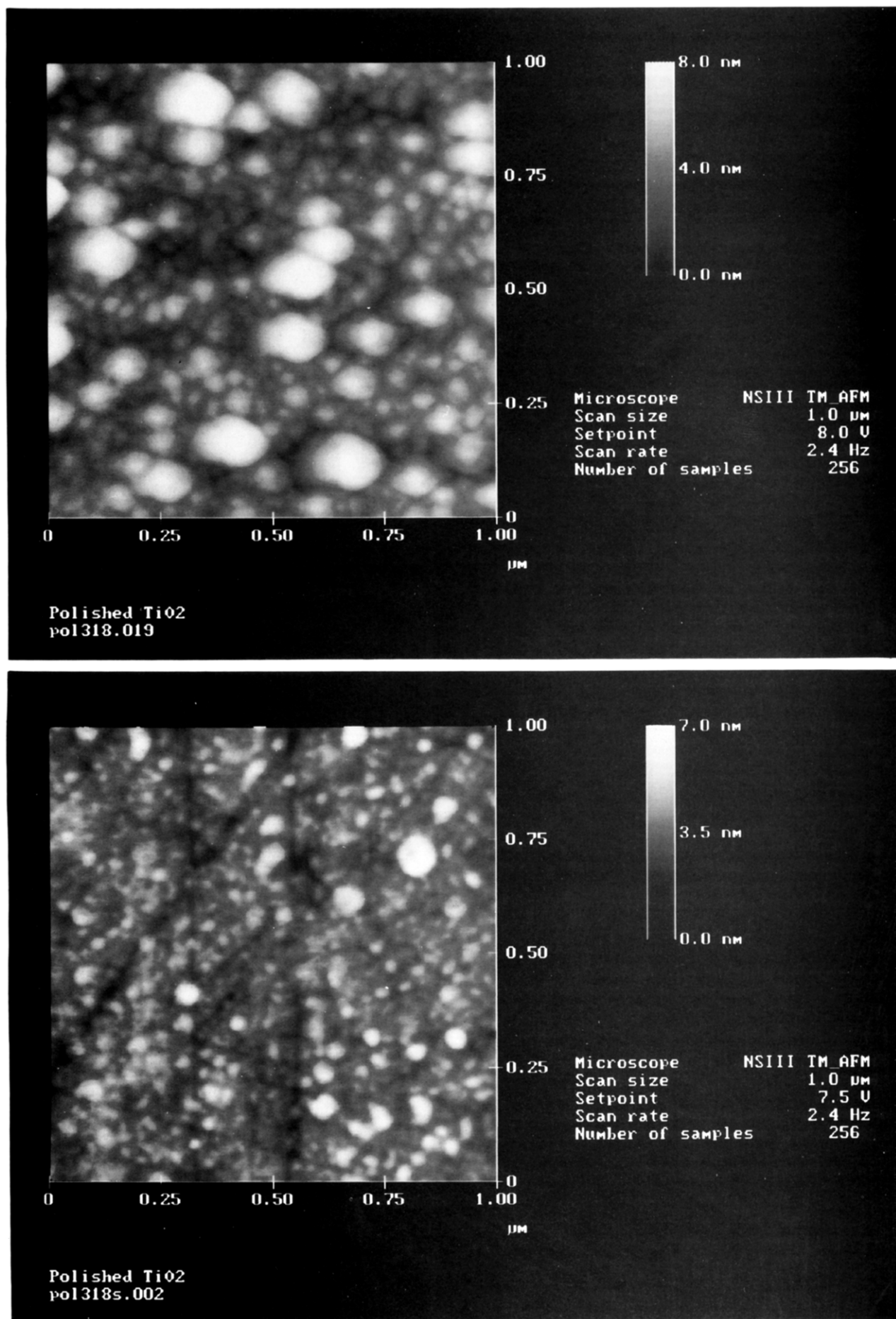


**Figure 2.** AFM images of TiO<sub>2</sub>(001) diamond polished surfaces: (a, top) 1 μm × 1 μm area; (b, bottom) 1 μm × 1 μm area exhibiting polishing scratches.

Table 1

TiO <sub>2</sub> surface (no. of images)	rms roughness (Å)	z range (Å)	surface area increase (%)
polished-showing particles (10)	9.2 ± 2.6	69 ± 16	0.46 ± 0.32
polished-showing scratches (25)	5.4 ± 1.5	49 ± 16	0.36 ± 0.29
argon-ion bombarded (47)	6.3 ± 1.9	47 ± 13	0.40 ± 0.22
750 K {011}-faceted (50)	8.9 ± 2.4	78 ± 25	0.91 ± 0.42
950 K {114}-faceted (50)	9.7 ± 2.1	73 ± 17	1.2 ± 0.35

Post-image processing of the images consisted of removal of sample tilt by calculating the least-squares fit for each scan line and then subtracting it from the raw data. Key image parameters include the *z* range, which is the difference between the highest and lowest vertical positions in the image. The rms roughnesses of the surfaces imaged were also determined. Rms roughness is the standard deviation of the *z* values within the image area. The surface area of the image, which represents the three-dimensional area, was calculated by taking the sum of the area of all triangles formed by three adjacent data points.

All UHV experiments were performed in a stainless steel, ion-pumped chamber. The UHV system was equipped with a Princeton Research Instruments Model 8-120 rear-view LEED optics, a single-pass cylindrical mirror analyzer, an electron source for collecting Auger spectra, and a mass spectrometer. The base pressure in the instrument was  $5 \times 10^{-10}$  Torr and was maintained by ion pumping.

The (001)-oriented TiO<sub>2</sub> single-crystal sample (5 mm × 5 mm × 0.5 mm) was obtained from Commercial Crystal Laboratories, Inc. The crystal was polished to a mirror finish with 0.25- $\mu$ m diamond paste and then rinsed ultrasonically with acetone in the laboratory atmosphere for at least 30 min. AFM imaging of samples rinsed for less than 15 min indicated that the sample surface was contaminated with residue from the diamond paste; 0.25- $\mu$ m particles were observed on the surface with the AFM in such cases.

The TiO<sub>2</sub>(001) single crystal was mounted on a sample stub that permitted the crystal to be heated in vacuum as well as removed from the UHV chamber for AFM imaging. The sample stub was fabricated from stainless steel. The crystal was mounted to a tantalum foil backing plate (0.127 mm thick) and was held in place by tantalum clips. The tantalum backing plate was spot welded to the sample stub. Behind the backing plate, inset in the stub was a tantalum wire (0.25- $\mu$ m diameter) coil which allowed for resistive heating of the sample. The coil was held in place and insulated from the stub and backing plate with high-temperature ceramic glue (Aremco Ultra-Temp 516). A diagram of the sample stub design is shown in Figure 1. The sample stub could be introduced to the chamber using a sample transfer device consisting of a magnetic linear/rotary drive terminated with a sample transfer fork. The sample transfer device was pumped with a turbomolecular pump and the sample was transferred from it to the UHV chamber through a gate valve. The sample was transferred from the transfer fork using a wobble stick (Thermionics) with *r*, *z*, and  $\theta$  motions.

The manipulator is a modified PHI Model 10-502 specimen manipulator which allowed 360° rotation of the sample to face the different instruments in the UHV chamber. From an assembly mounted on the manipulator extended a molybdenum rod encased in a ceramic tube which in turn was encased in a stainless steel tube. The sample stub was designed to slide over this covered rod (see Figure 1). Current was supplied to the sample stub resistive heater through the molybdenum rod. The heating rate was controlled by an IBM compatible PC interfaced with a Lambda power supply. The sample temperature was measured by a chromel-alumel thermocouple that was mounted with high-temperature cement to a plate in front of the mass spectrometer ionizer. The sample was brought into physical contact with the thermocouple before heating.

The TiO<sub>2</sub>(001) sample was cleaned in vacuum by repeated cycles of argon ion bombardment followed by annealing. A typical ion bombardment consisted of using a 3.5-keV argon ion beam, for a fixed time, with the angle of the incident beam at about 20° relative to the plane of the surface. Argon (Matheson ultrapure)

was introduced to the vacuum chamber through the gun and controlled manually by a variable leak valve. The pressure in the chamber was  $1 \times 10^{-5}$  Torr during ion bombardment. All parameters, once adjusted, were held constant during all subsequent sputtering experiments.

Samples were annealed for fixed time increments. Samples were routinely annealed to temperatures of ca. 750 and 950 K. At these temperatures thermal rearrangements to the {011}- and {114}-faceted structures, respectively, are known to occur.<sup>5</sup> LEED patterns for both structures obtained after annealing were consistent with those reported by Firment<sup>1</sup> for the "low-temperature" and "high-temperature" phases, respectively.

Typical production of a faceted surface proceeded as follows: The TiO<sub>2</sub>(001) single crystal was introduced to the UHV chamber using the sample transfer device described above. The sample was then argon-ion-bombarded for 60 min. The crystal temperature was then ramped to 750 K. The Auger spectrum was measured to check for the presence of surface carbon. The cycle was repeated until no appreciable carbon was detected. After a clean surface was obtained the crystal was annealed at 750 or 950 K for 30–60 min. LEED confirmed the faceted structure of the surface. The crystal was then removed from the UHV chamber using the sample transfer device for AFM imaging in air.

## Results

**Polished Surface.** AFM images of a TiO<sub>2</sub>(001) surface after diamond polishing are shown in Figure 2. Images of the polished surfaces showed the greatest variety of structures. These structures could be classified into two distinct categories: (a) particle-like features and (b) polishing scratches. Figure 2a shows an image dominated by particle-like features which range in size from 50 to 150 nm. These particle-like domains most resembled the faceted and ion-bombarded surfaces in appearance. However, these features on polished surfaces were larger and less uniform in size than those seen on the other surfaces. Surfaces of this type had an average rms roughness of 9.2 Å and an average *z* range of 69 Å. A summary of the roughness and surface area analyses for the different surfaces examined is contained in Table 1. All roughness, *z* range, and surface area values reported are based on 500 nm × 500 nm sampling areas.

The surface in Figure 2a was characterized by an rms roughness of 11 Å, and thus was one of the rougher surfaces examined according to Table 1. On polished surfaces with lower rms roughnesses it was sometimes possible to discern in the AFM images scratches resulting from the polishing process. One such example is shown in Figure 2b. The scratches in this image are 140–180 Å in width and 25–60 Å in depth. Scratches were the most distinct features seen on the polished surfaces. The scratches were not as wide as the nominal diameter of the diamond polishing grit (ca. 0.25  $\mu$ m), suggesting that they were caused by edges and corners of the abrasive particles, rather than by surfaces with dimensions approaching the particle diameter. With the exception of such scratches, surfaces like those in Figure 2b were quite flat and smooth. The surface imaged in Figure 2b had a rms roughness of 5.0 Å. Images of polished surfaces showing primarily polishing scratches had an average rms roughness of 5.4 Å and an average *z* range of 49 Å.

**{011}-Faceted TiO<sub>2</sub>(001) Surface.** The {011}-faceted surface was prepared by ramping the temperature of the crystal to 750 K after the crystal had been argon-ion bombarded, and annealing the crystal at that temperature for 60–90 min. Confirmation of the faceted structure was made by comparing LEED patterns with those of Firment.<sup>1</sup> AFM images of the {011}-faceted surface are shown in



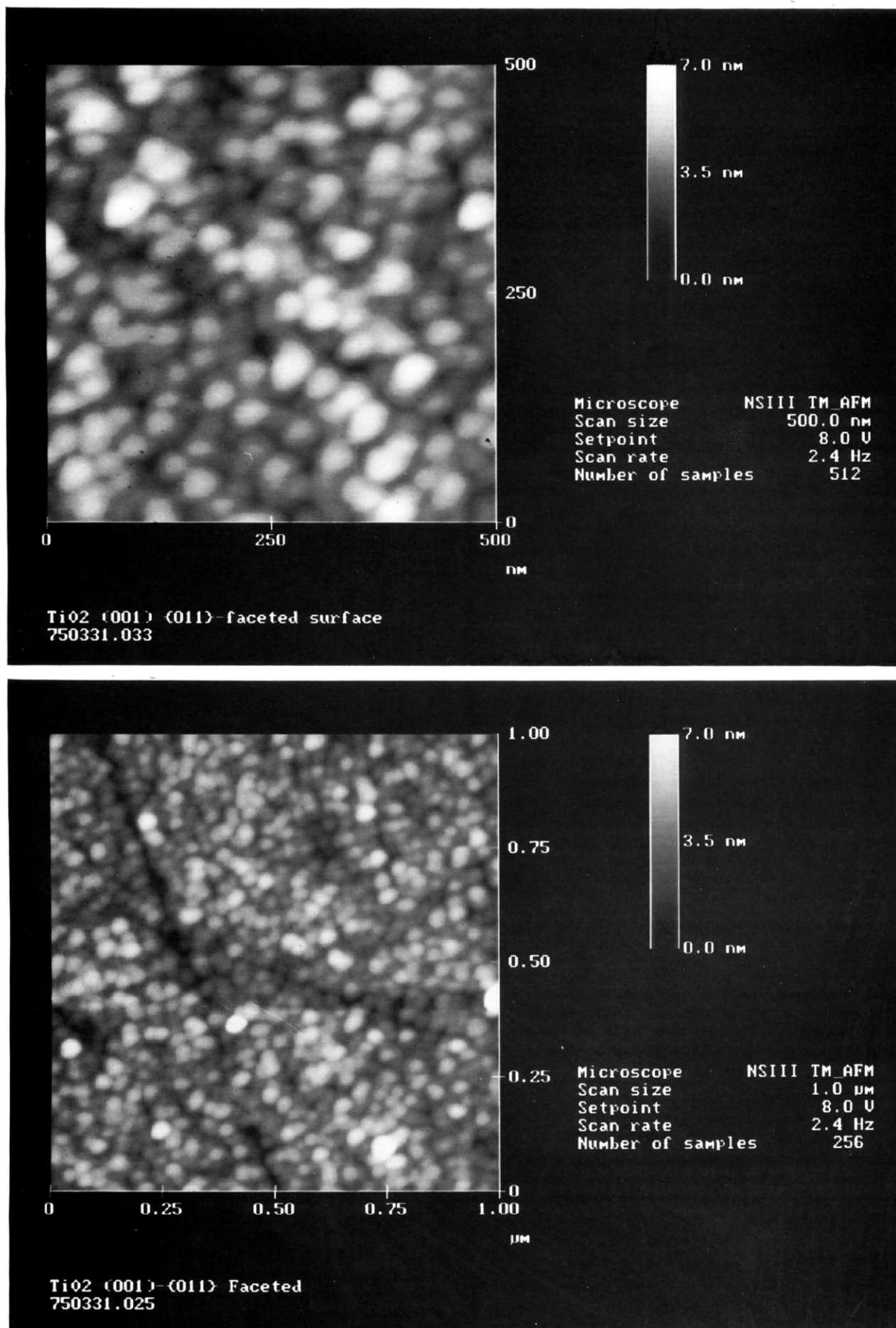


**Figure 3.** AFM images of TiO<sub>2</sub>(001)-{011}-faceted surfaces: (a, top) 500 nm × 500 nm area. (b, bottom) 1 μm × 1 μm area exhibiting scratches.

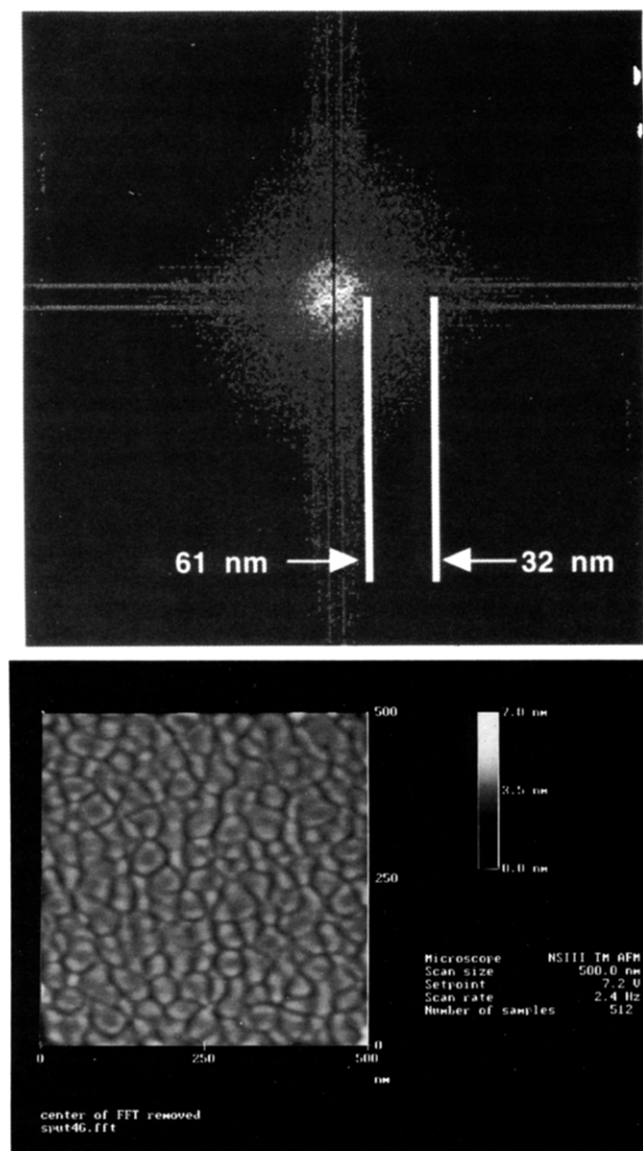


**Figure 4.** (a, top) FFT of an argon-ion sputtered surface. (b, bottom) Image of argon-sputtered surface back transformed from the FFT, retaining only the Fourier components corresponding to the annular region in (a).

Figure 3. The transformation of the polished surface to the {011}-faceted surface is quite striking. The latter surface is composed of domains of fairly regular size. Figure 3b shows an image in which a polishing scratch is still evident after repeated ion bombardment/annealing cycles. While the scratch remains, the image does show areas in which the scratch has been filled in by the domains observed throughout the rest of the image. The {011}-faceted surfaces were very flat; the average rms roughness was found to be 8.9 Å and the surface area increase was less than 1% relative to a flat surface. The average  $z$  range was 78 Å. The appearance of the surface and the size ranges of the domains did not change with different annealing times between and 1 and 3.5 h, the maximum annealing time utilized.

Since these surface images were composed arrays of similarly sized domains, fast Fourier transform (FFT) analysis of the images was used to determine the size range of the domains. For example, Figure 4a shows a 2-D FFT of an AFM image of an argon-ion-bombarded surface. The most notable feature of the FFT was the gray annulus centered about the origin. This frequency domain in

Fourier space corresponds to the range of facet sizes on the surface in real space. A ring (without azimuthal variation) forms because the domains have no preferred azimuthal orientation in the plane of the surface. The inner diameter of the ring represents the maximum domain size and the outer diameter, the minimum size in frequency space. Figure 4b illustrates the relationship between the real space image and the FFT. Figure 4b was created by removing all of the Fourier components of the FFT except those found within the gray annulus seen in Figure 4a and then transforming back to real space. The image in Figure 4b clearly shows how the annulus in Fourier space defines the boundaries of the domains and thus reflects their size range. FFT analysis of the images indicated that, for the {011}-faceted surface, the domains ranged in size from ca. 24 to 63 nm with an average size of 40 nm.

**{114}-Faceted  $\text{TiO}_2(001)$  Surface.** The {114}-faceted surface was prepared by ramping the temperature of the crystal to 950 K after the crystal had been argon-ion bombarded, and annealing the crystal at that temperature for 1–3.5 h. Confirmation of the faceted structure was made by comparing LEED patterns with those of Firmit.<sup>1</sup> These surfaces were also very flat; the average rms roughness was found to be 9.7 Å and the surface area increase was less than 1.2%. The average  $z$  range of the {114}-faceted surfaces was 73 Å. A representative AFM image of the {114}-faceted surface is shown in Figure 5. The {114}-faceted surface exhibited a distribution of domain sizes between 21 and 75 nm. The surface in Figure 5 appeared to have a slightly greater population of smaller domains than the {011}-faceted surface in Figure 3. No significant changes in the images were observed for faceted surfaces annealed for up to 3.5 h.

**Argon-Ion-Bombarded Surface.**  $\text{TiO}_2(001)$  surfaces were sputtered for 60 min at 3.5 keV in  $1 \times 10^{-5}$  Torr of argon. An image of  $\text{TiO}_2(001)$  surface after argon-ion bombardment of the {011}-faceted surface is shown in Figure 6. In all cases these surfaces showed no LEED pattern. Clearly visible in the image is an array of domain structures reminiscent of the structures seen on the {011}-faceted surface. The structures vary in shape from rectangular to circular and have a range of dimensions from 32 to 61 nm. The average rms roughness of these surfaces was 6.3 Å, comparable to that of the {011}-faceted surface. The similarity of the sputtered surface images to its well-ordered precursor demonstrates the minor changes caused by sputtering to surface morphology on the length scale of the domains.

## Discussion

This study illustrates the use of AFM to quantify the changes in surface morphology of  $\text{TiO}_2(001)$  through the use of roughness and surface area analysis. One of the advantages of AFM over other surface probe microscopies, such as STM, is that direct vertical measurements of the surface are obtainable. In STM, accurate  $z$ -dimension data are often difficult to acquire due to the convolution of geometric and electronic contributions to the vertical contrast of the images. STM does offer the advantage of easier implementation in the UHV environment. Ex situ AFM measurements such as those reported here do suffer from the fact that the surface, once removed from the UHV environment may be covered with a contamination layer of, e.g., water, carbon, and organics. In principle, however, by using the tapping mode technique the weakly

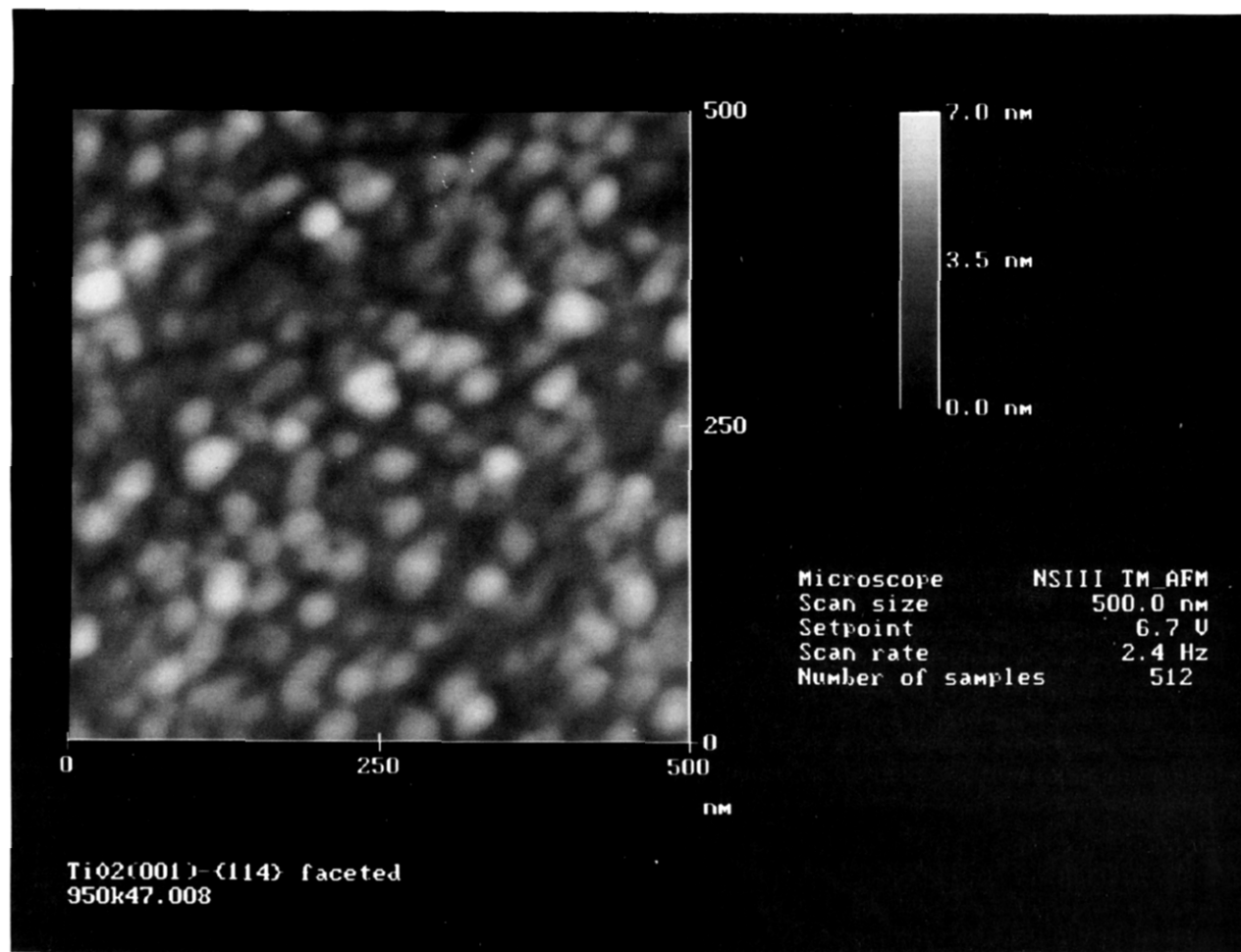


Figure 5. AFM image of a TiO<sub>2</sub>(001)-{114}-faceted surface; 500 nm × 500 nm area.

physisorbed contamination layer should not contribute significantly to the topography seen in an AFM image.<sup>26</sup> By oscillation of the tip at high enough amplitudes, the tip penetrates through the contamination layer, briefly contacting the surface of interest. Thus only the surface is responsible for the topography seen in the images. Contact AFM can also negate the effect of the surface overlayer, but less reliably.<sup>26</sup> By initially scanning the tip at sufficiently high applied forces, the tip may sweep away the weakly adsorbed overlayer.<sup>26</sup>

As with all probe microscopies, the presence of tip artifacts may hamper image interpretation. It is well-established that AFM images are a convolution of the tip shape and the sample topography and this interrelation can lead to artifact.<sup>27</sup> One such artifact occurs when the surface has features which are smaller than the radius of curvature of the tip apex. When this occurs, the AFM images represent primarily tip topography and not the sample surface of interest. For the surfaces imaged in this study, the primary features seen in the AFM images ranged in size from 20 to 80 nm. Radii of curvature of these features normal to the surface plane, calculated from individual line scans according to the method suggested by Westra et al.,<sup>27</sup> were approximately 3 times their characteristic lateral dimension, i.e., ca. 80–200 nm. These

radii values are much larger than the 10-nm radius<sup>28</sup> of the tapping mode AFM tip and therefore satisfy the criteria<sup>27</sup> for exclusion of this type of artifact.

The size range of the {011}-faceted structures reported here is in rough agreement with those reported by Poirier et al.<sup>22</sup> and by Lad and Antonik.<sup>23</sup> This work, along with the previous SPM studies, establishes a range of domain sizes between 100<sup>22</sup> and 240–650 Å for the {011}-faceted surface. The range of domain sizes for the {114}-faceted surface was found to be 210–750 Å. However, the domains observed by SPM are much larger than the unit cell dimensions of the faceted structures: 5.46 × 9.18 Å for the {011}-faceted structure and 6.49 × 13.3 Å for the {114} structure, deduced from the periodicity of the LEED patterns for the two surfaces.<sup>1</sup>

The structure of the {011} facets with (2 × 1) periodicities proposed by Firment would exhibit a repeat distance of 9.18 Å along the [010] direction. The {114} facets are tilted with respect to the (001) plane in the structure proposed by Firment.<sup>1</sup> This structure would produce a periodic variation of the surface height with an amplitude of 2.04 Å and a repeat distance of 13.3 Å along the [22̄1] axis. Features on this scale are not resolved in the AFM images presented, as they are below the lateral resolution of tapping mode AFM. The large domains imaged may be interpreted as flat regions on the order of 50–150 unit-cell lengths on a side, within which the surface exhibits the periodicities defined by the LEED patterns. This inter-

(26) Zhong, Q.; Inniss, D.; Kjoller, K.; Elings, V. B. *Surf. Sci.* 1993, 190, L688.

(27) Westra, K. L.; Mitchell, A. W.; Thomson, D. J. *J. Appl. Phys.* 1993, 74, 3608.

(28) Digital Instruments, Santa Barbara, CA.

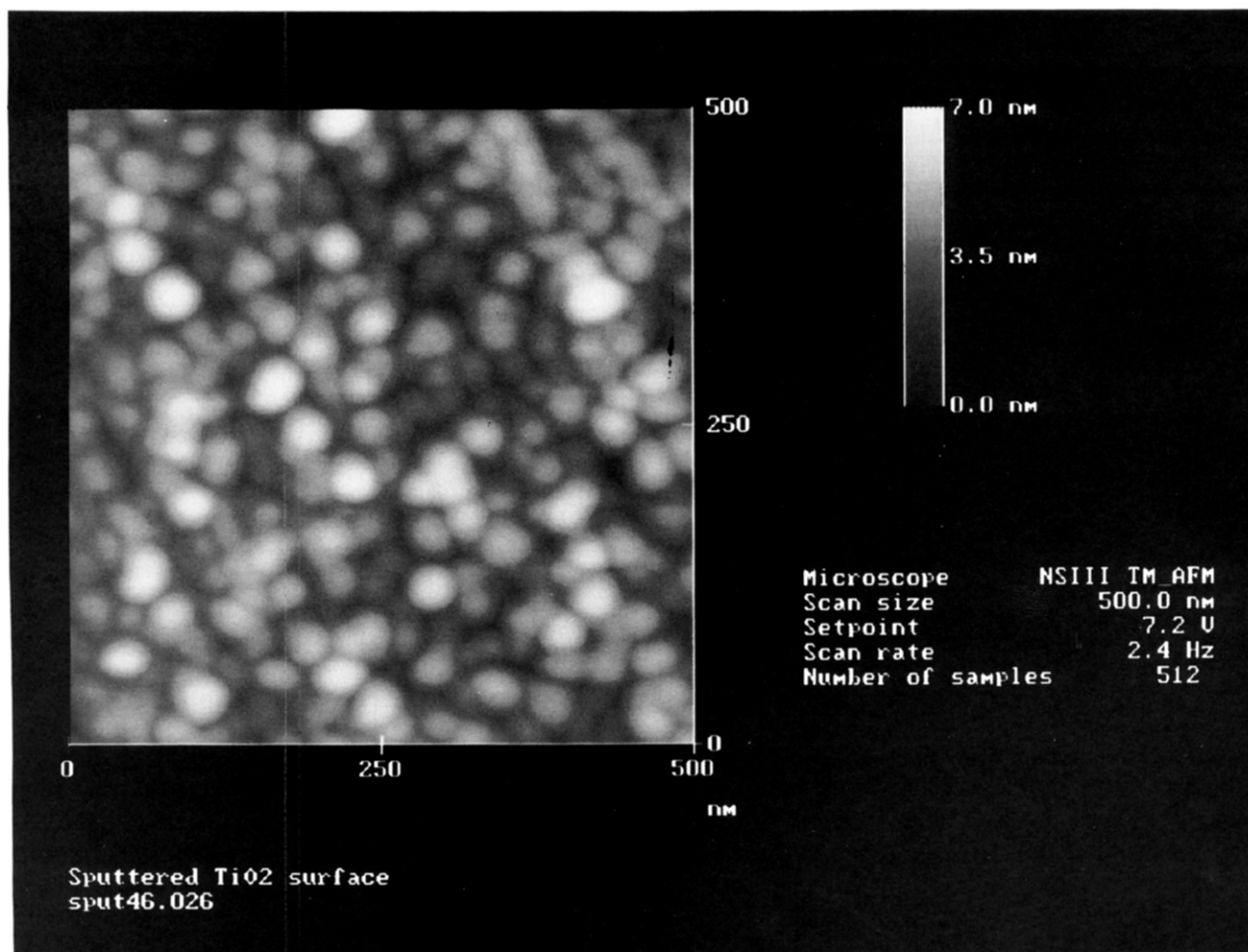


Figure 6. AFM image of a TiO<sub>2</sub>(001) argon-ion-sputtered surface; 500 nm × 500 nm area.

pretation is consistent with the STM observations and analysis by Poirier et al.<sup>22</sup> Those workers also interpreted their images as plateaus and hillocks with lateral dimensions up to 500 Å, terminated primarily by the faceted crystal planes proposed by Firment.<sup>1</sup>

In contrast to the STM images of TiO<sub>2</sub>(001) by Poirier et al.,<sup>20</sup> the AFM images reported here show the surface to be completely covered with discrete plateaus. The STM images of Poirier et al. show the surface to be composed of large faceted structures (plateaus) as well; however, significant regions of the surface were amorphous in structure. This difference in reported surface morphology is consistent with the LEED patterns observed. Poirier et al. reported diffuse LEED spots (several millimeters in diameter) on "low temperature" or "phase I" TiO<sub>2</sub>(001), whereas LEED patterns recorded in this study for the "phase I" (TiO<sub>2</sub>(001)-{011} faceted) surface as well as the "high temperature" or "phase II" (TiO<sub>2</sub>(001)-{114} faceted) surface were quite sharp, consistent with the absence of topographically distinct regions in the AFM images. Such differences in surface morphology are likely the result of the different annealing histories of the two single crystal samples.

The present results illustrate the effects on surface topography of mechanical polishing, argon ion bombardment, and annealing. Mechanical polishing, in general, produced larger, flatter domains than those observed on annealed surfaces, although the polished surfaces exhibited scratches from the diamond polishing paste. Other features seen on the polished surfaces included domain

structures whose sizes were several times larger than the plateaus observed on the annealed surfaces.

Surface treatments such as argon ion bombardment and annealing clearly alter the local structure of the surface, and thus the periodicity of the surface within the typical coherence length of LEED (ca. 100 Å). UHV STM studies of ion-bombarded metal surfaces clearly show how the surface topography is changed by sputtering.<sup>29</sup> These images show vacancies and islands one atomic layer in height with lateral dimensions from the atomic scale up to 30 Å. Such atomic scale changes in surface structure are below the resolution limit of the tapping mode AFM tip. However, the present results do demonstrate that the flat domains formed on the surface with lateral dimensions on the order of 500 Å are not altered significantly in size or shape by ion bombardment or annealing; changes in surface topography on this scale were not detected. Thus all of the surfaces exhibited considerable topographic uniformity on this scale.

As noted above, this investigation of the surfaces of TiO<sub>2</sub>(001) was motivated by the observation of a number of carbon-carbon bond forming reactions which are sensitive to surface properties. High selectivities for reactions which are sensitive to specific surface structures or oxidation states requires either that the surface be quite uniform or that other types of surface sites be much less reactive than those which produce the desired reaction. This work illustrates the uniformity of single crystal TiO<sub>2</sub> surfaces,

(29) Michely, T.; Comsa, G. *Phys. Rev. B* 1991, 44, 8411.

even those disordered by ion bombardment. All of the faceted and ion-bombarded surfaces imaged had rms roughness values less than 10 Å. The surface areas of all of the TiO<sub>2</sub> surfaces were less than 1.2% greater than an ideally flat surface. If one assumes, for example, typical domains of 100 × 100 × 1 unit cell high, as appear in the AFM images, the concentration of "edge" sites would also be of the order of 2-4% of the total. Given this level of uniformity, the high selectivities observed for some reactions (e.g., 90% selectivity for the cyclotrimerization of 2-butyne<sup>19</sup>) on reduced surfaces is less surprising. These results further illustrate the application of metal oxide single-crystal surfaces that are unstable and facet, to probe the structural dependence and site requirements of surface reactions.

### Conclusions

TiO<sub>2</sub>(001) surfaces active for a variety of organic reactions in UHV were imaged by AFM. Once formed,

large flat domain structures with lateral dimensions of ca. 500 Å were not changed significantly by annealing and argon-ion bombardment, although changes in surface structure within these flat domains were detectable by LEED. All surfaces treated in UHV exhibited average rms roughnesses of less than 10 Å and total *z*-range variation of less than 100 Å. Overall these surfaces were found to be very smooth and flat. The topographic uniformity of these surfaces with changes in local cation coordination and oxidation state allows the preparation of different surfaces which provide active and selective sites for various carbon-carbon bond-forming reactions with different site requirements.

**Acknowledgment.** We gratefully acknowledge the support of the National Science Foundation (Grant CTS 9100404) for support of this research. The scanning probe microscopes employed were acquired via an equipment grant from the U.S. Department of Energy.